EuroIntervention 2019;15:692-699 published online March 2019

The influence of multidirectional shear stress on plaque progression and composition changes in human coronary arteries

Annette M. Kok[1], MSc; David S. Molony[2], PhD; Lucas H. Timmins[3], PhD; Yi-An Ko[4], PhD; Eric Boersma[1], PhD; Parham Eshtehardi[2], MD; Jolanda J. Wentzel[1]*, PhD; Habib Samady[2], MD

1. Department of Cardiology, Biomedical Engineering, Erasmus MC, Rotterdam, the Netherlands; 2. Department of Medicine, Emory University School of Medicine, Atlanta, GA, USA; 3. Department of Bioengineering, University of Utah, Salt Lake City, UT, USA; 4. Department of Biostatistics and Bioinformatics, Emory University Rollins School of Public Health, Atlanta, GA, USA

J.J. Wentzel and H. Samady contributed equally to this manuscript.

This paper also includes supplementary data published online at: https://eurointervention.pcronline.com/doi/10.4244/EIJ-D-18-00529

KEYWORDS

- clinical research
- intravascular ultrasound
- NSTEMI

Abstract

Aims: Local wall shear stress (WSS) plays an important role in the onset of atherosclerotic plaque formation; however, it does not fully explain plaque progression and destabilisation. We aimed to investigate for the first time the influence of multidirectional WSS features on plaque progression and plaque composition changes in human coronary arteries.

Methods and results: Coronary artery imaging using biplane angiography and virtual histology intravascular ultrasound (VH-IVUS) was performed in twenty patients with coronary artery disease at baseline and after six-month follow-up. Three-dimensional surfaces of the coronary arteries were generated using the coronary imaging and, together with patient-specific flow measurements, different WSS features (multidirectional and conventional time-averaged WSS [TAWSS]) were determined at baseline using computational fluid dynamics (CFD). The changes in plaque component area over the six-month period were determined from VH-IVUS. Changes in plaque composition rather than plaque size were primarily associated with the (multidirectional) WSS at baseline. Interestingly, regions simultaneously exposed to low TAWSS and low multidirectional WSS showed the greatest plaque progression ($p<0.001$).

Conclusions: In this patient study, several multidirectional WSS features were found to contribute significantly to coronary plaque progression and changes in plaque composition.

**Corresponding author: Cardiology Department, Biomedical Engineering, Room Ee2338, Erasmus MC, PO Box 2040, 3000 CA Rotterdam, the Netherlands. E-mail: j.wentzel@erasmusmc.nl*

SUBMITTED ON 10/05/2018 - REVISION RECEIVED ON 1st 20/09/2018 / 2nd 05/12/2018 / 3rd 05/02/2019 - ACCEPTED ON 06/03/2019

DOI: 10.4244/EIJ-D-18-00529

Abbreviations

CFD	computational fluid dynamics
CFI	cross-flow index
DC	dense calcium
FF	fibro-fatty tissue
FT	fibrous tissue
LAD	left anterior descending
LME	linear mixed effect
NC	necrotic core
OSI	oscillatory shear index
RRT	relative residence time
TAWSS	time-averaged wall shear stress
transWSS	transverse wall shear stress
VH-IVUS	virtual histology intravascular ultrasound
WSS	wall shear stress

Introduction

Atherosclerotic plaques develop in regions exposed to low and oscillatory blood flow-induced wall shear stress (WSS)[1,2]. Low WSS creates a pro-atherogenic environment and is therefore involved in plaque initiation by stimulating the endothelial expression of pro-inflammatory genes and proteins[3]. Furthermore, WSS is recognised for its role in plaque growth and changes in plaque composition towards a high-risk vulnerable plaque[4-6].

However, the magnitude of WSS is insufficient to predict plaque growth or plaque compositional changes fully[7]. Multidirectional WSS is a measure for change in the direction of the shear stress during the cardiac cycle. Therefore, Peiffer et al suggested that multidirectional WSS may also be important in lesion development[8]. From the biological point of view, multidirectional WSS affects endothelial cell morphology and function. Upon exposure to laminar flow, the endothelial cells align with the favourable main flow/WSS direction, which is related to the induction of atheroprotective signalling pathways. In contrast, multidirectional WSS can cause cell inability to align, which in turn is associated with induction of inflammatory pathways[9,10].

Transverse WSS (transWSS), a new multidirectional WSS metric, may be important in atherosclerosis development. TransWSS is the WSS magnitude perpendicular to the main flow direction[8]. Regions with high transWSS co-localised with lipid deposition in rabbits[8], but its effect on plaque progression and plaque composition changes is unknown. The same holds true for the normalised transWSS (cross-flow index [CFI][11] and other well-known multidirectional WSS metrics, oscillatory shear index [OSI] and relative residence time [RRT][12]).

To the best of our knowledge this is the first study to investigate the clinical relevance of transWSS and other multidirectional WSS metrics on progression and destabilisation of atherosclerosis in human coronary arteries in a longitudinal study.

Editorial, see page 656

Methods

SUBJECTS

From December 2007 to January 2009, twenty patients presented to the catheterisation laboratory at Emory University Hospital with either an abnormal non-invasive stress test or stable angina syndrome. An invasive physiological evaluation of a non-obstructive lesion was performed. All patients received optimal medical therapy including 80 mg atorvastatin daily. The inclusion and exclusion criteria were described previously[6]. After six months, a repeat catheterisation was performed to assess changes in plaque morphology. In each patient the most proximal part of the left anterior descending (LAD) artery was investigated. The study complied with the Declaration of Helsinki and was approved by the Emory University Institutional Review Board. Each patient provided written informed consent.

IMAGING ACQUISITION AND RECONSTRUCTION

The left coronary arteries were visualised using biplane angiography (Philips Medical Systems, Andover, MA, USA). From these images, back projection image analysis (QAngio XA 3D RE; Medis, Leiden, the Netherlands) was used to determine the catheter path. Doppler-derived velocity measurements were performed in the left main coronary artery using the ComboWire® (Volcano Corporation, Rancho Cordova, CA, USA). To obtain detailed lumen and vessel wall composition information, virtual histology intravascular imaging (VH-IVUS) was performed using a phased-array 20 MHz Eagle Eye® Gold catheter (Volcano Corporation) **(Figure 1A)**. The pullback speed was 0.5 mm·s^{-1}; ECG gating was performed at the peak of the r-wave. The VH-IVUS pullback length was at least 60 mm and contained at least two side branches, which were later used as landmarks for the three-dimensional (3D) geometry reconstruction. In some cases, a shorter region was imaged and in several cases 3D reconstruction of the full 60 mm was not possible due to severe vessel overlapping in the angiography images. Based on fusion information from the different imaging modalities, the left coronary artery was 3D reconstructed, including the left main coronary artery and major side branches[13].

COMPUTATIONAL FLUID DYNAMICS AND ANALYSIS

Computational fluid dynamics (CFD) was applied to perform transient WSS calculations (ANSYS Fluent 15; ANSYS, Inc., Canonsburg, PA, USA) in this 3D reconstruction **(Figure 1B-Figure 1D)**[14]. As flow input, 80% of the instantaneous peak velocity measured by the ComboWire was chosen arbitrarily (as a rounded midpoint between 50 and 100%). The flow was imposed as a plug profile at the inlet to represent the aorta plug-like velocity. All the other outlets were assumed to be pressure-free. In addition to the time-averaged WSS (TAWSS), the OSI, RRT, transWSS and CFI were also calculated **(Supplementary Table 1)**. The differences in these parameters are shown in **Supplementary Figure 1**.

The acquired VH-IVUS images were exported from the VH-analysis software (echoPlaque 4.0; INDEC Medical Systems, Inc., Los Altos, CA, USA) and imported into a custom MATLAB subroutine to determine the composition and plaque area. The RGB pixel values, which are distinct across the four VH-IVUS identified plaque components (fibrous tissue [FT], fibro-fatty

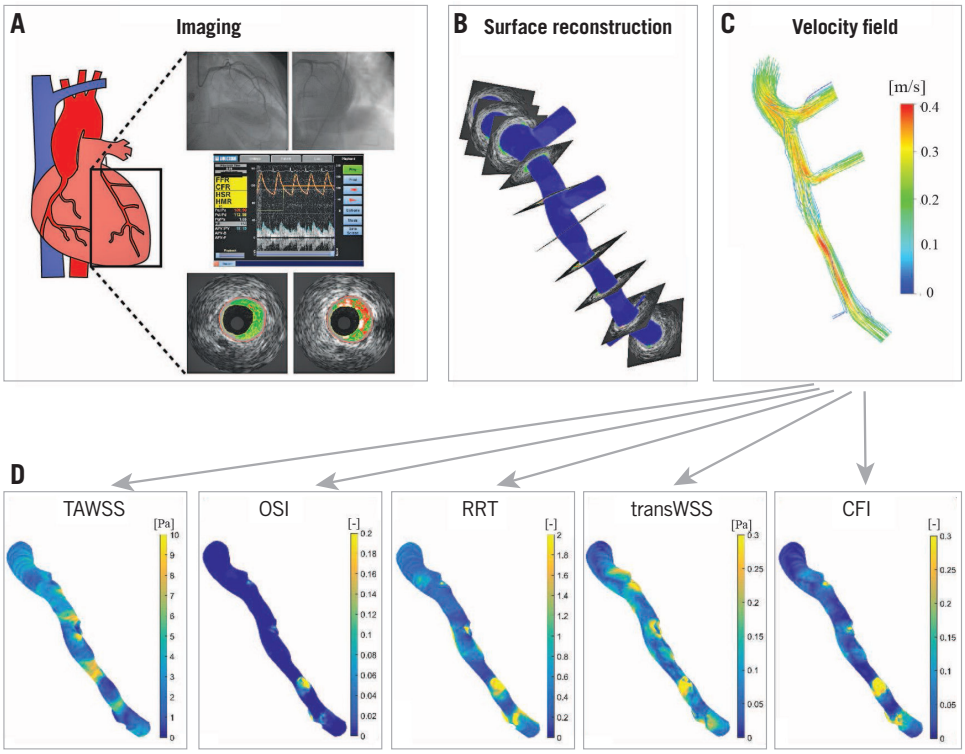

Figure 1. *Schematic overview of the methods. A) Biplane angiography, Doppler-derived velocity measurements and virtual histology intravascular ultrasound (VH-IVUS). B) Lumen surface 3D reconstruction was obtained by stacking the VH-IVUS based lumen contours perpendicular to the biplane angiography-derived 3D centreline. Local velocities (C) and multidirectional WSS metrics (time-averaged wall shear stress [TAWSS], oscillatory shear index [OSI], relative residence time [RRT], cross-flow index [CFI] and transverse wall shear stress [transWSS]) (D) were determined using computational fluid dynamics.*

tissue [FF], necrotic core [NC], and dense calcium [DC]), were identified per cross-section.

The registration of baseline and follow-up IVUS was performed by a single expert investigator (P. Eshtehardi), who used a standardised protocol to identify landmarks (side branches and large calcific regions)[15]. Furthermore, the spacing between the IVUS images is nearly equivalent (0.5 mm) which made matching between baseline and follow-up images even more straightforward. The circumferential co-registration between baseline and follow-up was done with an automated framework which yielded excellent results[16]. The multidirectional shear stress metrics and plaque changes over time were quantified over 45° 3-mm regions **(Figure 2)** for further analysis[13]. A detailed description of the CFD and the analysis is presented in **Supplementary Appendix 1-Supplementary Appendix 4**.

STATISTICAL ANALYSIS

Based on previous studies, the TAWSS data were divided into three groups: low (0-1 Pa), intermediate (1-2.5 Pa), and high (>2.5 Pa)[6]. Thresholds for pathological levels of transWSS or CFI have never been explored in human coronary arteries. Therefore, we divided

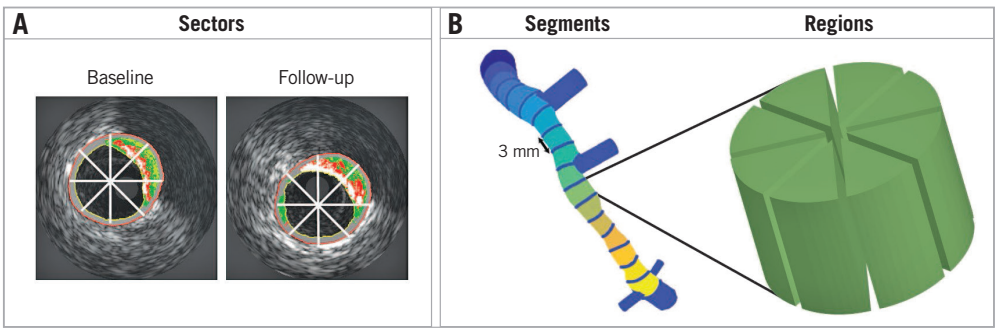

Figure 2. *Schematic representation of data analysis. A) Virtual histology intravascular ultrasound image at baseline and a matched image at follow-up. The white lines indicate the cross-sectional averaging in eight sectors (45°). B) 3 mm longitudinal averaging of the eight sectors leads to regions used in the final analysis.*

these metrics into three equally distributed groups (tertiles). This was also done for the RRT and OSI. A linear mixed-effects (LME) model was used to investigate the association between the WSS metric(s) (fixed effect) and plaque composition (dependent variable). The correlations between multiple plaque composition values are accounted for by using subject-specific random intercepts. This allows for varying intercepts for each patient. In addition to fitting separate models for individual (multidirectional) shear stress features (TAWSS, OSI, RRT, transWSS, CFI), we included the following covariates in the LME model: TAWSS, CFI and their interaction (to test for synergetic effects). The statistical analysis was performed in R, version 3.3.2 (R Foundation for Statistical Computing, Vienna, Austria) using the LME4 package; $p<0.05$ was considered significant.

Results

GENERAL DATA

Baseline characteristics of the twenty patients have been described previously **(Supplementary Table 2)**. In total, 1,846 VH-IVUS images were analysed with 107 (62.5-123) images per artery. From these images, 316 3-mm segments (18 [11-21] segments per artery) containing 2,488 regions (141 [86.5-165] regions per artery) were used for final analysis. The average values for the low, intermediate, and high categories of the different WSS parameters are presented in **Table 1**.

CONVENTIONAL SHEAR STRESS METRIC: TAWSS

Plaque area progression and composition changes were greatly influenced by exposure to baseline TAWSS. A significant inverse association between TAWSS and plaque progression (p=0.006) was observed, showing more plaque regression going from low TAWSS (–0.002±0.020 mm^2) towards intermediate (–0.027±0.018 mm^2) and high (–0.042±0.018 mm^2) TAWSS **(Figure 3, Supplementary Table 3)**. The other plaque constituents followed a similar significant decreasing pattern with increasing TAWSS. Significant differences were found between the low and high TAWSS groups of all the components except for FF tissue and NC.

Table 1. The number of regions and the median with interquartile range of the wall shear stress (WSS) metrics for each group (low, intermediate, and high). The WSS metrics include the time-averaged WSS (TAWSS), oscillatory shear index (OSI), relative residence time (RRT), cross-flow index (CFI) and transverse WSS (transWSS).

	Low	Intermediate	High
TAWSS regions, n	193	996	1,299
TAWSS magnitude [Pa]	0.78 (0.67-0.90)	1.65 (1.40-2.03)	3.69 (3.03-4.66)
OSI, RRT, CFI, transWSS regions, n	829	830	829
OSI·10^{-3} [–]	0.51 (0.25-0.85)	4.21 (2.61-6.91)	24.2 (16.4-42.4)
RRT [Pa^{-1}]	0.29 (0.23-0.37)	0.65 (0.56-0.74)	1.14 (0.95-1.60)
CFI [–]	0.03 (0.02-0.04)	0.08 (0.06-0.09)	0.16 (0.13-0.21)
transWSS [Pa]	0.06 (0.04-0.07)	0.11 (0.10-0.13)	0.18 (0.16-0.24)

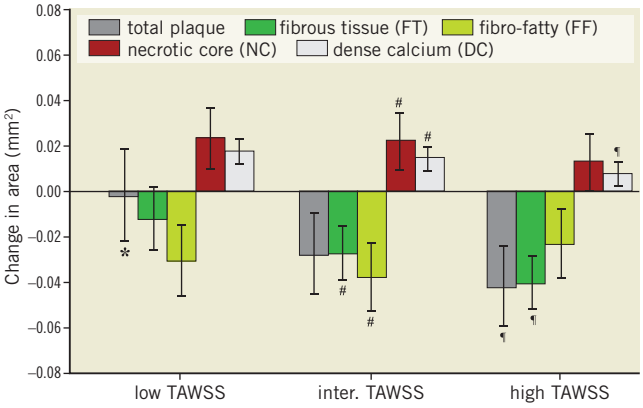

Figure 3. *Plaque area and composition changes over a six-month period for plaques exposed to low, intermediate and high time-averaged wall shear stress (TAWSS). Error bars are the standard error. p<0.05: low versus intermediate (*), intermediate versus high (#) and low versus high (¶).*

MULTIDIRECTIONAL SHEAR STRESS

In general, we observed that multidirectional WSS was primarily involved in altering the plaque composition rather than the plaque size. No significant difference in total plaque area changes was found in low vs high OSI regions **(Figure 4A)**. An inverse relationship with OSI was found for FF tissue (p<0.001), implying the higher the OSI the more FF tissue regression. Significantly higher progression was found for NC area (p=0.001) and DC area (p<0.001) in the high OSI regions compared to the intermediate and low OSI regions, but no differences were observed for FT regression in these regions. Evaluation of the changes in plaque exposed to low vs high RRT revealed that plaques exposed to low RRT exhibited more regression of total plaque area (p<0.001) and FT (p=0.003) than plaques that were exposed to high RRT **(Figure 4B)**. Similar to high OSI, high RRT regions showed more NC (p=0.008) and DC (p<0.001) progression and more regression of FF tissue (p=0.0003) than low RRT regions. A positive RRT relationship was found for DC (p<0.001) and FT (p=0.01), implying the higher the RRT the more DC progression and less FT tissue regression.

Different levels of transWSS did not significantly influence the total plaque growth, FT, and FF **(Figure 5A)**. Regions exposed to high transWSS showed more progression of NC area (p=0.01) and DC area (p<0.0001) than regions exposed to low transWSS. Similar patterns were seen for the CFI **(Figure 5B)**. Changes in total plaque area and FT were unaffected by different levels of CFI. There was a positive relation between CFI and the NC (p<0.002) and DC groups (p<0.001), and a negative relation for the FF tissue (p<0.001).

CO-LOCALISATION OF TAWSS AND MULTIDIRECTIONAL SHEAR STRESS

To study whether plaque progression is influenced by multidirectional WSS additional to TAWSS, regions of low and high TAWSS were co-localised with low, intermediate, and high

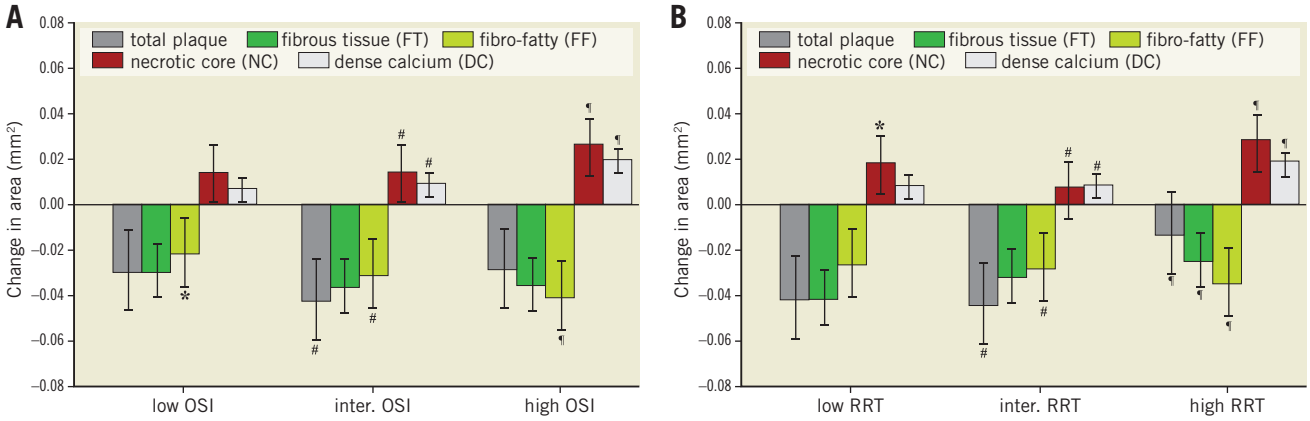

Figure 4. *Plaque area and composition changes over a six-month period for plaques exposed to low, intermediate and high oscillatory shear index (OSI) (A) and exposed to low, intermediate and high relative residence time (RRT) (B). Error bars are the standard error. p<0.05: low versus intermediate (*), intermediate versus high (#) and low versus high (¶).*

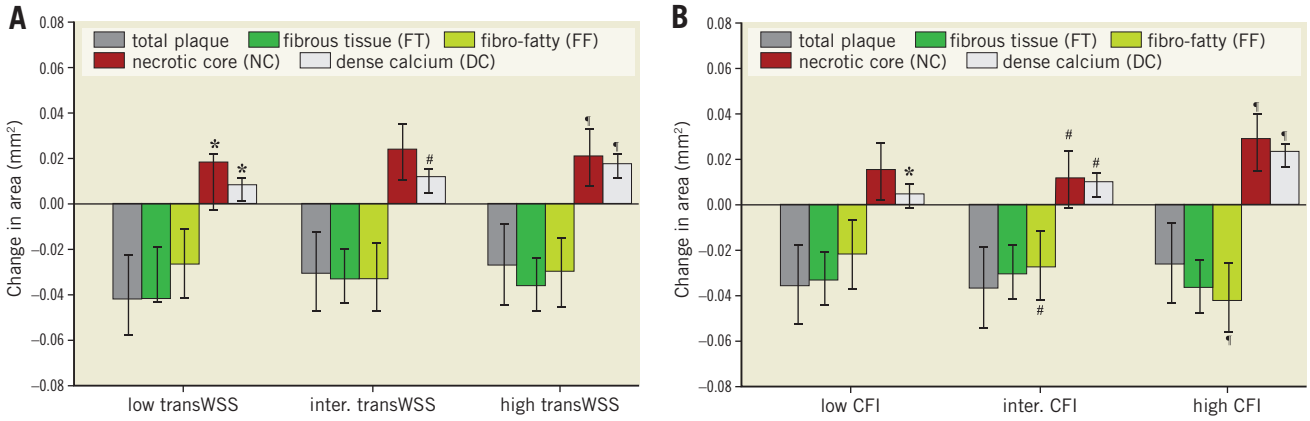

Figure 5. *Plaque area and composition changes over a six-month period for plaques exposed to low, intermediate and high transverse wall shear stress (transWSS) (A) and cross-flow index (CFI) (B). Error bars are the standard error. p<0.05: low versus intermediate (*), intermediate versus high (#) and low versus high (¶).*

multidirectional WSS. The greatest progression of total plaque, FT and FF area was found in regions of low TAWSS co-localised with low and intermediate CFI (low CFI: 0.15 mm^2, intermediate CFI: 0.10 mm^2), which was much larger than the average plaque growth in low TAWSS (–0.001 mm^2) **(Figure 3, Figure 6, Supplementary Table 4)**. Further, the change in area in these groups was significantly greater than the change in area in the low TAWSS regions co-localised with high CFI (total plaque, FT, FF: p<0.0001). High TAWSS regions co-localised with low or high CFI demonstrated the greatest NC progression, while in high CFI regions the greatest regression was found for total plaque area, FT, and FF tissue. In high TAWSS regions, plaque regression (p<0.001) was observed in all the CFI groups, which resulted from significant changes in the plaque components FT (p<0.001), FF tissue (p<0.001), NC (p<0.001), and DC (p<0.001). A significant synergetic effect was found for all the components (p<0.001).

The co-localisation of TAWSS with OSI **(Supplementary Figure 2, Supplementary Table 5)** showed a similar response to the co-localisation of TAWSS with CFI **(Figure 6)**. However, the co-localisation results with RRT showed similar results to TAWSS alone **(Supplementary Figure 3)**. Interestingly, in the co-localisation of high TAWSS with high RRT, plaque growth and plaque composition changes mimic more the high RRT response **(Supplementary Figure 3, Supplementary Table 6)**.

Discussion

For the first time, the effect of TAWSS together with multidirectional WSS on plaque progression and compositional changes was investigated in the coronary arteries of patients with coronary artery disease (CAD). We showed that multidirectional WSS mainly contributes to changes in plaque composition, such that plaque vulnerability is increased, and less to changes in plaque size. Interestingly, regions with low TAWSS co-localised with low to intermediate CFI resulted in the greatest plaque progression; low TAWSS alone did not show significant plaque progression **(Figure 3)**. High TAWSS, regardless of the CFI magnitude, was shown to influence characteristics of plaque vulnerability (i.e., total plaque area and FT regression, and NC progression).

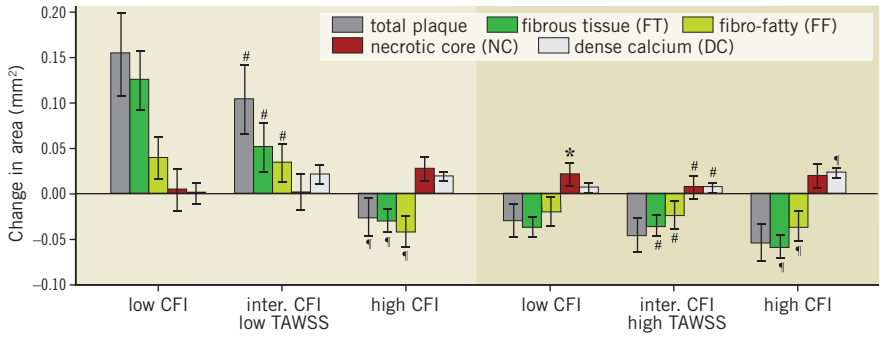

Figure 6. *Plaque area and composition changes over a six-month period for plaques exposed to low or high time-averaged wall shear stress (TAWSS) co-localised with low, intermediate and high cross-flow index (CFI). Error bars are the standard error. p<0.05: low versus intermediate (*), intermediate versus high (#) and low versus high (¶).*

TIME-AVERAGED WALL SHEAR STRESS

Our results on changes in plaque size and composition in regions with low and high TAWSS are in close agreement with previous studies[6]. It is under debate whether high-risk plaque development is associated with either low or high TAWSS[17,18]. We hypothesise that high TAWSS is atheroprotective in early atherosclerosis, but at later stages destabilises the plaque.

MULTIDIRECTIONAL SHEAR STRESS

Only one study has investigated the influence of multidirectional WSS on plaque progression and compositional changes in human coronary arteries[13]. This study measured oscillatory WSS as the maximum angle deviation of WSS over the cardiac cycle. Plaques that were exposed to low TAWSS co-localised with low oscillatory WSS showed large plaque progression whilst those which were co-localised with high oscillatory WSS showed transformation towards a vulnerable plaque phenotype. Both of these observations are in agreement with our study. However, that work did not address the individual effect of oscillatory WSS and the combined role of high TAWSS and multidirectional WSS in plaque progression and destabilisation[13].

The influence of OSI and RRT on plaque initiation has been investigated previously. In murine aortas, plaque location was in better agreement with OSI and RRT than TAWSS[19]. A study in human coronary arteries showed that plaques are often located at low TAWSS regions[20]; however, both high OSI and RRT were more predictive for the presence of plaque. A caveat to this study was that they virtually removed the plaque in order to represent the healthy state of the artery and assessed the TAWSS, OSI and RRT in this manipulated geometry. Therefore, this study cannot be regarded as a true natural history study and comparisons should be interpreted with caution. We found a more pronounced effect of RRT and OSI on changes in plaque composition than plaque growth. Specifically, regions with the largest progression of NC and DC and regression of FF tissue were associated with high OSI and RRT.

A recently introduced haemodynamic metric to characterise another feature of multidirectional flow is transverse WSS (transWSS) or normalised transWSS (CFI). The present study shows that there is no effect of transWSS or CFI on plaque progression; however, it appears to influence plaque composition. Indeed, a number of studies suggest that an increase in multidirectional flow or transWSS is atherogenic[9,21]. In an *in vitro* study, endothelial cells subjected to transverse flow resulted in an increase in inflammation (increase in expression of NF-κB)[9]. In another study using rabbits, high transWSS was found at lesion sites, whereas this correlation was less apparent with either TAWSS or OSI[21]. This relationship was less evident in more mature rabbits. However, they did not study plaque composition, which in our study proved to be most affected by the transWSS. It should be noted that these studies were performed using either cultured cells or atherosclerotic animal models and hence may not be fully representative of the human case.

CO-LOCALISATION OF TIME-AVERAGED WALL SHEAR STRESS WITH MULTIDIRECTIONAL SHEAR STRESS

We present here, for the first time, data on low and high TAWSS regions co-localised with various multidirectional WSS parameters. In contrast to the low TAWSS, the plaque changes in the high TAWSS regions seem not so much influenced by the multidirectional WSS. Co-localisation of TAWSS with CFI and OSI showed the same patterns in plaque progression, which was expected because of the high correlation between these parameters (r=0.83).

Our data on plaque progression potentially suffer from regression-to-the-mean effects. This was investigated in a separate analysis by incorporating baseline plaque area into the LME model. We observed that plaque progression was still significantly related to all multidirectional WSS parameters. However, although still significant, it was less pronounced in the low TAWSS co-localised with low CFI regions. Therefore, the conclusions are all valid.

Limitations

All patients were treated with high doses of statins. With this therapy, an overall plaque regression is often observed. Therefore, the results that we obtained are a balance of pro-atherogenic haemodynamic conditions, e.g., low TAWSS, and the anti-atherogenic influence of statins. With current treatment strategy in CAD patients, these data reflect WSS-related plaque progression in this population.

Furthermore, our data on the relationship between plaque progression and (multidirectional) WSS were obtained in LAD arteries only. Although no data exist on possible differences in WSS-related plaque progression in the other coronary arteries, it cannot be excluded that the multidirectional WSS in these arteries has a larger range and therefore shows a different response.

VH-IVUS was used to assess the local plaque composition; however, VH-IVUS is under debate for its applicability to identify local plaque composition. Although some studies showed a moderate correlation between VH-IVUS and histology especially for the FF and NC tissue[22,23], a number of studies showed >80% accuracy to identify FT, FF, NC, and DC compared to histology[24]. Therefore, in general, the relationships found between plaque components and multidirectional WSS reflect the actual changes in the tissue. However, conclusions with regard to FF and NC should be interpreted with caution.

The number of patients studied is limited. Therefore, multiple regions within a single coronary artery were analysed. To obtain independent samples, the data were averaged over 3 mm and circumferentially over 45°[7,14]. We opted for 45° sectors to ensure minimal loss in earlier observed details in the haemodynamic environment simultaneously with the highest possible accuracy in circumferential matching with follow-up data[13,14]. The circumferential registration algorithm showed a matching error of <10° in 78% of the cross-sections compared to manual image registration. This means that, of these cross-sections, 78%-100% of the sector was correctly matched. To account further for subject dependencies, for data analysis a sophisticated LME regression model was used. Using this approach, we obtained statistical significance, despite the limited number of patients. Besides, this study is an exploratory study and therefore the conclusions should be confirmed in a larger patient database.

Because we defined low TAWSS as <1 Pa, in the co-localisation analysis we ended up with a low number of regions exposed to both low TAWSS and low CFI (n=11) and low TAWSS and intermediate CFI (n=15), contrasting with the other groups in which at least 167 data points were present, possibly due to different boundary conditions as compared to previous studies[7]. Splitting the TAWSS data into tertiles would have resulted in a larger number of data points but would not have allowed studying the co-localisation with true low TAWSS. Despite the fact that these sample sizes were low, the statistics revealed strong effects in these regions.

Conclusions

In conclusion, this study shows that there are important associations between (multidirectional) WSS metrics and changes in plaque composition reflecting increased plaque destabilisation. Further, multidirectional flow acts synergistically with TAWSS on plaque composition and plaque size. Therefore, the combination of (multidirectional) WSS profiling and plaque imaging in combination with systemic risk factors is imperative to identify plaques that potentially develop into a vulnerable plaque.

Impact on daily practice

Our data confirmed that TAWSS is a good predictor for locations of plaque growth. On top of that, multidirectional WSS provides information on changes in plaque composition and potentially detects regions with plaque destabilisation. Therefore, we recommend using both the TAWSS and one of the multidirectional WSS parameters. We suggest that the multidirectional parameter would be either OSI or CFI, since RRT and transWSS are dependent on TAWSS.

Funding

Funding was received from the European Research Council under the European Union's Seventh Framework Programme/ERC Grant Agreement n. 310457 and Vereniging Trustfonds Erasmus Universiteit Rotterdam.

Conflict of interest statement

A. Kok reports grants from the European Research Council and from Trustfonds during the conduct of the study. H. Samady reports grants and personal fees from Philips Volcano, grants from Abbott Vascular and Medtronic, during the conduct of the study, and other from SIG and Covanos, outside the submitted work. H. Samady and D. Molony have a patent pending for Methods and Systems for Determining Hemodynamic Information for One or More Arterial Segments. J. Wentzel reports a grant from the European Research Council during the conduct of the study. The other authors have no conflicts of interest to declare.

References

1. Pedersen EM, Oyre S, Agerbæk M, Kristensen IB, Ringgaard S, Boesiger P, Paaske WP. Distribution of early atherosclerotic lesions in the human abdominal aorta correlates with wall shear stresses measured in vivo. *Eur J Vasc Endovasc Surg.* 1999;18:328-33.

2. Stone PH, Coskun AU, Kinlay S, Clark ME, Sonka M, Wahle A, Ilegbusi OJ, Yeghiazarians Y, Popma JJ, Orav J, Kuntz RE, Feldman CL. Effect of endothelial shear stress on the progression of coronary artery disease, vascular remodeling, and in-stent restenosis in humans: in vivo 6-month follow-up study. *Circulation.* 2003;108:438-44.

3. Zhou J, Li YS, Chien S. Shear stress-initiated signaling and its regulation of endothelial function. *Arterioscler Thromb Vasc Biol.* 2014;34:2191-8.

4. Chatzizisis YS, Baker AB, Sukhova GK, Koskinas KC, Papafaklis MI, Beigel R, Jonas M, Coskun AU, Stone BV, Maynard C, Shi GP, Libby P, Feldman CL, Edelman ER, Stone PH. Augmented expression and activity of extracellular matrix-degrading enzymes in regions of low endothelial shear stress colocalize with coronary atheromata with thin fibrous caps in pigs. *Circulation.* 2011;123:621-30.

5. Vergallo R, Papafaklis MI, Yonetsu T, Bourantas CV, Andreou I, Wang Z, Fujimoto JG, McNulty I, Lee H, Biasucci LM, Crea F, Feldman CL, Michalis LK, Stone PH, Jang IK. Endothelial shear stress and coronary plaque characteristics in humans: combined frequency-domain optical coherence tomography and computational fluid dynamics study. *Circ Cardiovasc Imaging.* 2014;7:905-11.

6. Samady H, Eshtehardi P, McDaniel MC, Suo J, Dhawan SS, Maynard C, Timmins LH, Quyyumi AA, Giddens DP. Coronary artery wall shear stress is associated with progression and transformation of atherosclerotic plaque and arterial remodeling in patients with coronary artery disease. *Circulation.* 2011;124:779-88.

7. Stone PH, Saito S, Takahashi S, Makita Y, Nakamura S, Kawasaki T, Takahashi A, Katsuki T, Nakamura S, Namiki A, Hirohata A, Matsumura T, Yamazaki S, Yokoi H, Tanaka S, Otsuji S, Yoshimachi F, Honye J, Harwood D, Reitman M, Coskun AU, Papafaklis MI, Feldman CL; PREDICTION Investigators. Prediction of progression of coronary artery disease and clinical outcomes using vascular profiling of endothelial shear stress and arterial plaque characteristics: the PREDICTION study. *Circulation.* 2012;126:172-81.

8. Peiffer V, Sherwin SJ, Weinberg PD. Computation in the rabbit aorta of a new metric – the transverse wall shear stress – to quantify the multidirectional character of disturbed blood flow. *J Biomech.* 2013;46:2651-8.

9. Wang C, Baker BM, Chen CS, Schwartz MA. Endothelial cell sensing of flow direction. *Arterioscler Thromb Vasc Biol.* 2013;33:2130-6.

10. Baeyens N, Mulligan-Kehoe MJ, Corti F, Simon DD, Ross TD, Rhodes JM, Wang TZ, Mejean CO, Simons M, Humphrey J, Schwartz MA. Syndecan 4 is required for endothelial alignment in flow and atheroprotective signaling. *Proc Natl Acad Sci U S A.* 2014;111:17308-13.

11. Mohamied Y, Sherwin SJ, Weinberg PD. Understanding the Fluid Mechanics Behind Transverse Wall Shear Stress. *J Biomech.* 2017;50:102-9.

12. Himburg HA, Grzybowski DM, Hazel AL, LaMack JA, Li XM, Friedman MH. Spatial comparison between wall shear stress measures and porcine arterial endothelial permeability. *Am J Physiol Heart Circ Physiol.* 2004;286:1916-22.

13. Timmins LH, Molony DS, Eshtehardi P, McDaniel C, Oshinski JN, Giddens DP, Samady H. Oscillatory wall shear stress is a dominant flow characteristic affecting lesion progression patterns and plaque vulnerability in patients with coronary artery disease. *J R Soc Interface.* 2017 Feb:14(127).

14. Timmins LH, Molony DS, Eshtehardi P, McDaniel MC, Oshinski JN, Samady H, Giddens DP. Focal association between wall shear stress and clinical coronary artery disease progression. *Ann Biomed Eng.* 2015;43:94-106.

15. Mintz GS, Garcia-Garcia HM, Nicholls SJ, Weissman NJ, Bruining N, Crowe T, Tardif JC, Serruys PW. Clinical expert consensus document on standards for acquisition, measurement and reporting of intravascular ultrasound regression/progression studies. *EuroIntervention.* 2011;6:1123-30.

16. Timmins LH, Suever JD, Eshtehardi P, McDaniel MC, Oshinski JN, Samady H, Giddens DP. Framework to co-register longitudinal virtual histology-intravascular ultrasound data in the circumferential direction. *IEEE Trans Med Imaging.* 2013;32:1989-96.

17. Eshtehardi P, Brown AJ, Bhargava A, Costopoulos C, Hung OY, Corban MT, Hosseini H, Gogas BD, Giddens DP, Samady H. High wall shear stress and high-risk plaque: an emerging concept. *Int J Cardiovasc Imaging.* 2017;33:1089-99.

18. Koskinas KC, Feldman CL, Chatzizisis YS, Coskun AU, Jonas M, Maynard C, Baker AB, Papafaklis MI, Edelman ER, Stone PH. Natural history of experimental coronary atherosclerosis and vascular remodeling in relation to endothelial shear stress: a serial, in vivo intravascular ultrasound study. *Circulation.* 2010;121:2092-101.

19. Hoi Y, Zhou YQ, Zhang X, Henkelman RM, Steinman DA. Correlation between local hemodynamics and lesion distribution in a novel aortic regurgitation murine model of atherosclerosis. *Ann Biomed Eng.* 2011;39:1414-22.

20. Rikhtegar F, Knight JA, Olgac U, Saur SC, Poulikakos D, Marshall W, Cattin PC, Alkadhi H, Kurtcuoglu V. Choosing the optimal wall shear parameter for the prediction of plaque location-A patient-specific computational study in human left coronary arteries. *Atherosclerosis.* 2012;221:432-7.

21. Mohamied Y, Rowland EM, Bailey EL, Sherwin SJ, Schwartz MA, Weinberg PD. Change of direction in the biomechanics of atherosclerosis. *Ann Biomed Eng.* 2015;43:16-25.

22. Granada JF, Wallace-Bradley D, Win HK, Alviar CL, Builes A, Lev EI, Barrios R, Schulz DG, Raizner AE, Kaluza GL. In vivo plaque characterization using intravascular ultrasound-virtual histology in a porcine model of complex coronary lesions. *Arterioscler Thromb Vasc Biol.* 2007;27:387-93.

23. Thim T, Hagensen MK, Wallace-Bradley D, Granada JF, Kaluza GL, Drouet L, Paaske WP, Bøtker HE, Falk E. Unreliable assessment of necrotic core by virtual histology intravascular ultrasound in porcine coronary artery disease. *Circ Cardiovasc Imaging.* 2010;3:384-91.

24. Nasu K, Tsuchikane E, Katoh O, Vince DG, Virmani R, Surmely JF, Murata A, Takeda Y, Ito T, Ehara M, Matsubara T, Terashima M, Suzuki T. Accuracy of in vivo coronary plaque morphology assessment: a validation study of in vivo virtual histology compared with in vitro histopathology. *J Am Coll Cardiol.* 2006;47:2405-12.

Supplementary data

Supplementary Appendix 1. Detailed methodology.

Supplementary Appendix 2. Computational fluid dynamics.

Supplementary Appendix 3. Metrics to describe shear stress features.

Supplementary Appendix 4. Analysis.

Supplementary Figure 1. A schematic overview of three different situations of different shear stress patterns.

Supplementary Figure 2. Change in plaque area and composition over a six-month period for plaques exposed to low or high time-averaged wall shear stress (TAWSS) co-localised with low, intermediate and high oscillatory shear index (OSI).

Supplementary Figure 3. Change in plaque area and composition over a six-month period for plaques exposed to low or high time-averaged wall shear stress (TAWSS) co-localised with low, intermediate and high relative residence time (RRT).

Supplementary Table 1. A mathematical description of the shear stress metrics.

Supplementary Table 2. Patient demographic and clinical characteristics.

Supplementary Table 3. Change in plaque area and composition (±the standard error) over a six-month period for plaques exposed to low, intermediate and high time-averaged wall shear stress (TAWSS), oscillatory shear index (OSI), relative residence time (RRT), cross-flow index (CFI) and transverse wall shear stress (transWSS).

Supplementary Table 4. Change in plaque area and composition (±the standard error) over a six-month period for plaques exposed to low or high time-averaged wall shear stress (TAWSS) co-localised with low, intermediate and high cross-flow index.

Supplementary Table 5. Change in plaque area and composition (±the standard error) over a six-month period for plaques exposed to low or high time-averaged wall shear stress (TAWSS) co-localised with low, intermediate and high oscillatory shear index (OSI).

Supplementary Table 6. Change in plaque area and composition (±the standard error) over a six-month period for plaques exposed to low or high time-averaged wall shear stress (TAWSS) co-localised with low, intermediate and high relative residence time (RRT).

The supplementary data are published online at: https://eurointervention.pcronline.com/doi/10.4244/EIJ-D-18-00529

Supplementary data

Supplementary Appendix 1. Detailed methodology

The greyscale images and the radiofrequency data were stored for offline analysis. The lumen and external elastic membrane were segmented by an experienced reader with echoPlaque, version 4.0 (INDEC Medical Systems, Santa Clara, CA, USA). High intra-observer reproducibility was found for the segmentation of the total plaque area (concordance correlation coefficient [CCC]=0.968) and the necrotic core area (CCC=0.978). The segmented contours were perpendicularly stacked upon the catheter path. The exact location of the contours on the catheter path was determined from the pullback speed of the catheter. The left main coronary artery and major side branches were included in the 3D reconstruction as cylindrical extensions with a diameter based on IVUS images and the orientation was extracted from biplane angiography [12]. An attempt was made to include all side branches that were visible on IVUS. Flow extensions were added to the inlet (one diameter) and all the outlets (seven diameters) [12]. Next, the 3D surface was created by connecting the IVUS contours and the side branches using non-uniform rational b-splines (Geomagic Studio 11, Research Triangle Park, NC, USA) **(Figure 1B)**.

Supplementary Appendix 2. Computational fluid dynamics

To allow computational fluid dynamics (CFD), a volume mesh was created with ICEM CFD (ANSYS 15; ANSYS, Inc., Canonsburg, PA, USA). To extract the instantaneous mean velocity from the instantaneous peak velocity measured by the ComboWire a conversion factor is needed. For a parabolic profile this conversion factor is 50%; however, our velocity profiles are between parabolic and flat, therefore we chose 80%. This instantaneous mean velocity was imposed as a plug profile at the inlet to represent the aorta plug-like velocity. All the other outlets were assumed to be pressure-free. Our decision to employ pressure-free boundary conditions is a result of extensive investigation which indicates that the resulting computed flow-field best reproduces the *in vivo* haemodynamic environment.

The blood was assumed to behave as an incompressible Newtonian fluid (ρ=1.06 g/cm^3, μ=3.5 cP). Unsteady flow simulations were performed in Fluent (ANSYS 15). Three cardiac cycles were simulated and only the last cycle was used in our analysis. Each cardiac cycle consisted of 300 time steps. The shear stress vector at each mesh node was exported every 10 time steps for further analysis. A typical example of velocity streamlines, as calculated by CFD, is depicted in **Figure 1C**. Post-processing was performed with

the Vascular Modelling Toolkit (http://www.vmtk.org/) and MATLAB, version 2015a (MathWorks Inc., Natick, MA, USA).

Supplementary Appendix 3. Metrics to describe shear stress features

In addition to the conventional TAWSS, several other metrics to describe features of multidirectional flow were derived from the CFD computed velocity field (i.e., oscillatory shear index [OSI], relative residence time [RRT], transverse wall shear stress [transWSS], and cross-flow index [CFI]). The mathematical expression of these parameters is shown in **Supplementary Table 1**. The OSI quantifies the oscillatory behaviour of the normalised shear stress by taking the forward and backward direction into consideration. RRT can be interpreted as the time that particles spend in one distinct area near the arterial wall; the greater the RRT the more interaction with the arterial wall. TransWSS determines the amount of flow perpendicular to the main flow direction. TransWSS is dependent on the shear stress magnitude. To study the effect of multidirectional flow alone, the transWSS was normalised by the instantaneous shear stress. This metric is called the cross-flow index (CFI) [11]. A representative example for each of the shear stress metrics is given in **Figure 1D**.

Supplementary Appendix 4. Analysis

The acquired VH-IVUS images were exported from the VH-analysis software (echoPlaque 4.0) and imported into a custom MATLAB subroutine to determine the composition and plaque area. The RGB pixel values, which are distinct across the four VH-IVUS identified plaque components (fibrous tissue [FT], fibro-fatty tissue [FF], necrotic core [NC], and dense calcium [DC]), were identified and quantified for each eight 45° sectors **(Figure 2A)** [12]. The shear stress analysis was performed by a single investigator (L.H. Timmins) blinded to the IVUS data. The registration of baseline and follow-up IVUS was performed by another single expert investigator (P. Eshtehardi), who used a standardised protocol to identify landmarks (side branches and large calcific regions). Furthermore, the spacing between the IVUS images is nearly equivalent (0.5 mm) which made matching between baseline and follow-up images even more straightforward. However, the heart rate at baseline and follow-up is not necessarily the same; this leads to small differences in spacing between the images. Therefore, some baseline images correspond with two follow-up images (2% of the data). In this case, the average area of the IVUS-VH derived components was taken. Longitudinal mismatch because of vessel elongation and changes in tortuosity are not expected in a six-month period.

The circumferential co-registration between baseline and follow-up was done with an automated framework which yielded excellent results [15]. The change in area of each plaque component was defined as the follow-up area minus the baseline area in each sector. We averaged the change in area over 3-mm segments (six IVUS images) to ensure that the data points were independent in the longitudinal direction **(Figure 2B)**. Each averaged sector within the 3-mm segments is hereafter referred to as a region.

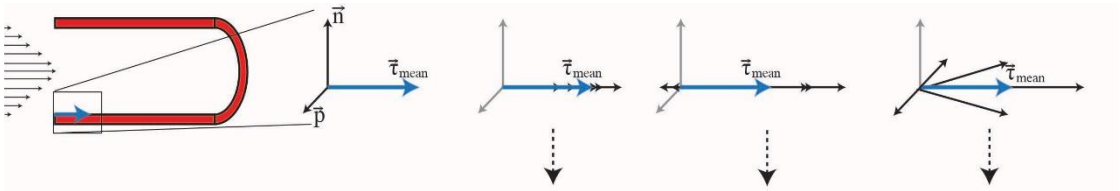

SS parameter	Case 1	Case 2	Case 3
TAWSS [Pa]	2	2	2
OSI [-]	0	0.07	0.12
RRT [Pa^{-1}]	0.5	0.58	0.66
transWSS [Pa]	0	0	0.8
CFI [-]	0	0	0.58

Supplementary Figure 1. A schematic overview of three different situations of different shear stress patterns.

In each pattern the time-averaged wall shear stress (TAWSS) is 2 Pa and is therefore constant. In each pattern the oscillatory shear index (OSI), relative residence time (RRT), cross-flow index (CFI) and transverse wall shear stress (transWSS) are calculated.

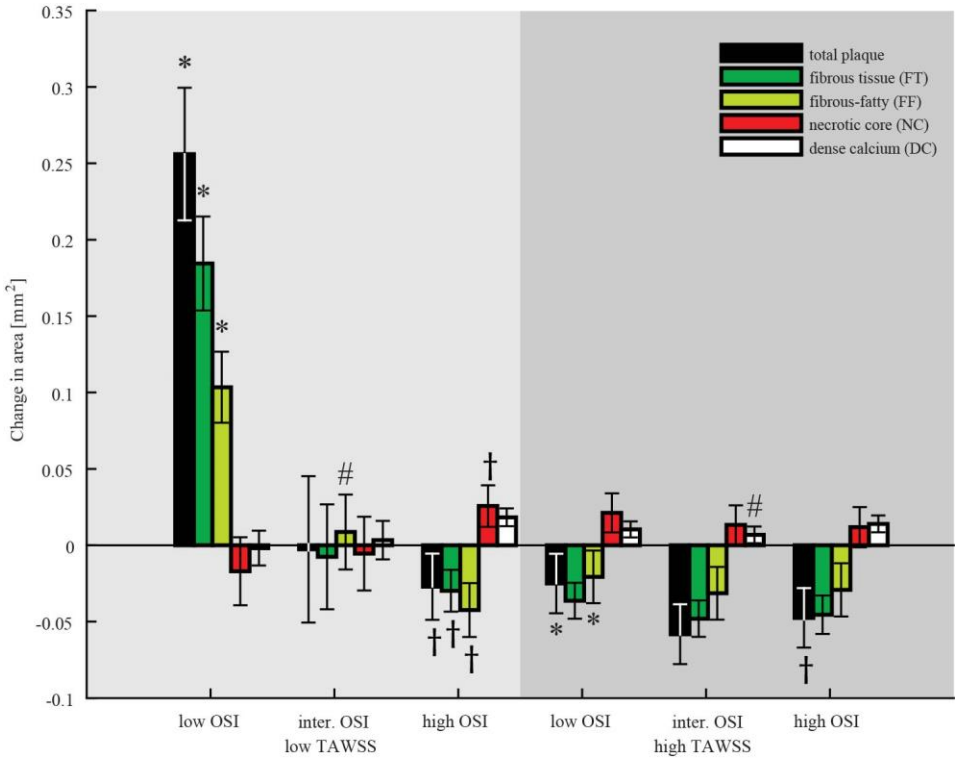

Supplementary Figure 2. Change in plaque area and composition over a six-month period for plaques exposed to low or high time-averaged wall shear stress (TAWSS) co-localised with low, intermediate and high oscillatory shear index (OSI).

Error bars are the standard error. p<0.05: low versus intermediate (*), intermediate versus high (#) and low versus high (†).

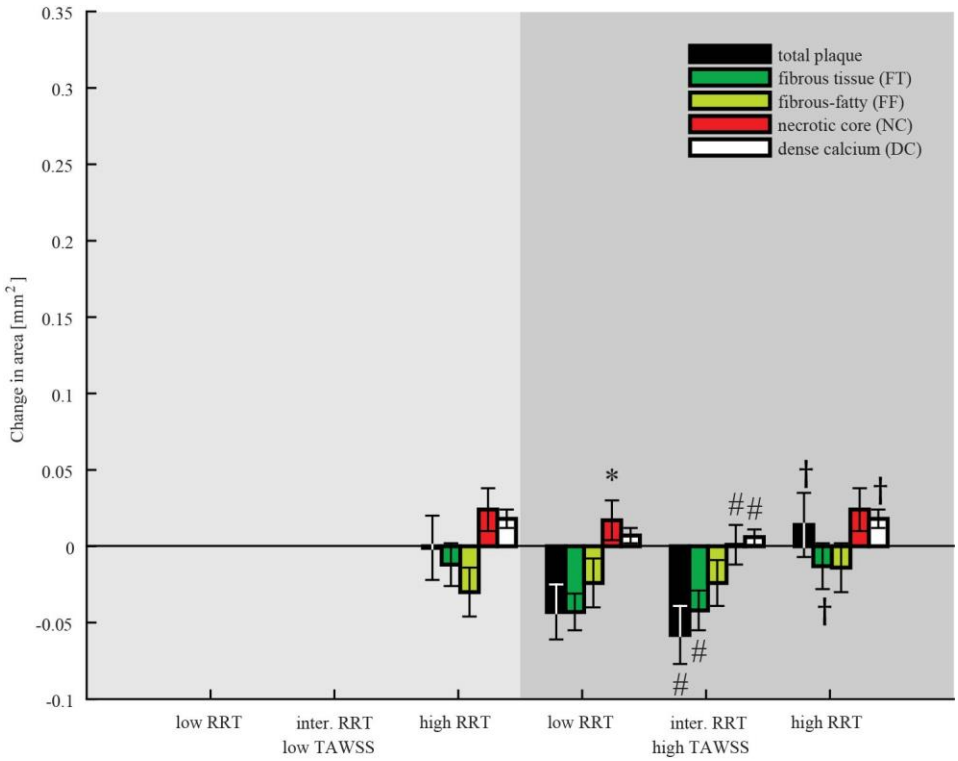

Supplementary Figure 3. Change in plaque area and composition over a six-month period for plaques exposed to low or high time-averaged wall shear stress (TAWSS) co-localised with low, intermediate and high relative residence time (RRT).

Error bars are the standard error. p<0.05: low versus intermediate (*), intermediate versus high (#) and low versus high (†).

Supplementary Table 1. A mathematical description of the shear stress metrics.

The time-averaged wall shear stress (TAWSS) averages the magnitude of the shear stress over the cardiac cycle. Oscillatory shear index (OSI) is a measure for oscillatory flow. Relative residence time (RRT) is a measure for time of a particle spent in a certain area. To calculate the transWSS first the vector normal to the surface ($n(x)$) and the vector in the average shear stress direction were calculated ($p(x)$). The transWSS is then obtained by averaging the shear stress magnitude in direction $p(x)$. The CFI is similar to the transWSS, the only difference being that it is normalised with the instantaneous shear stress vector. In this way the CFI becomes dimensionless. A schematic overview of the different situations of different shear stress patterns is shown in Supplementary Figure 1. This figure clearly shows that TAWSS does not capture the full nature of the multidirectional flow; different shear stress metrics are needed to capture different flow effects.

Supplementary Table 1. Mathematical description of the shear stress metrics.

Shear stress metric	Formula
Time-averaged wall shear stress (TAWSS), [Pa]	$\frac{1}{T}\int_0^T \lvert\tau_w(x,t)\rvert\, dt$
Oscillatory shear index (OSI), [-]	$0.5 \times \left(1 - \frac{\left\lvert\int_0^T \tau_w(x,t)\, dt\right\rvert}{\int_0^T \lvert\tau_w(x,t)\rvert\, dt}\right)$
Relative residence time (RRT), [Pa^{-1}]	$\approx \frac{1}{TAWSS(x) * \left(1 - 2 * OSI(x)\right)}$
Transverse wall shear stress (transWSS), [Pa]	$\frac{1}{T}\int_0^T \lvert\tau_w(x,t) \cdot p(x)\rvert\, dt$ With $p(x) = n(x) \times \frac{\frac{1}{T}\int_0^T \tau_w(x,t)\, dt}{\left\lvert\frac{1}{T}\int_0^T \tau_w(x,t)\, dt\right\rvert}$
Cross-flow index (CFI), [-]	$\frac{1}{T}\int_0^T \left\lvert\frac{\tau_w(x,t)}{\lvert\tau_w(x,t)\rvert} \cdot p(x)\right\rvert\, dt$

$\tau_w(x,t)$ is the instantaneous shear stress vector for each node x and time t. The cardiac cycle time is T. $p(x)$ is the vector perpendicular to the surface normal $n(x)$ and the mean wall shear stress vector.

Supplementary Table 2. Patient demographic and clinical characteristics.

Characteristic	All patients (n=20)
Age (years)	54 (46–68)
Male, n (%)	13 (65)
White, n (%)	14 (70)
Body mass index (kg m^{-1})	30 (27–36)
Hypertension, n (%)	14 (70)
Current smoking, n (%)	5 (25)
Diabetes mellitus, n (%)	7 (35)
Family history of CAD, n (%)	8 (40)
Previous myocardial infarction, n (%)	2 (10)
Coronary flow reserve	2.35 (2.03–2.59)
Fractional flow reserve	0.90 (0.82–0.96)
Baseline lipid profile	
Total cholesterol (mg dl^{-1})	186.0 (168.0–212.5)
Triglycerides (mg dl^{-1})	115.5 (83.5–158.8)
High-density lipoprotein (mg dl^{-1})	39.5 (33.3–52.8)
Low-density lipoprotein (mg dl^{-1})	118.5 (105.3–140.5)
C-reactive protein (mg l^{-1})	2.7 (1.5–7.2)
Follow-up lipid profile	
Total cholesterol (mg dl^{-1})	139.0 (124.3–151.3)
Triglycerides (mg dl^{-1})	107.0 (75.8–138.8)
High-density lipoprotein (mg dl^{-1})	42.5 (31.3–57.3)
Low-density lipoprotein (mg dl^{-1})	70.5 (54–87.5)

Continuous data are reported as median (interquartile range).

CAD: coronary artery disease

Supplementary Table 3. Change in plaque area and composition (±the standard error) over a six-month period for plaques exposed to low, intermediate and high time-averaged wall shear stress (TAWSS), oscillatory shear index (OSI), relative residence time (RRT), cross-flow index (CFI) and transverse wall shear stress (transWSS).

		Total plaque area (mm^2)	Fibrous tissue area (mm^2)	Fibrous-fatty area (mm^2)	Necrotic core area (mm^2)	Dense calcium area (mm^2)
TAWSS	Low	**-0.002±0.020***	-0.012±0.014	-0.030±0.016	0.023±0.013	0.018±0.006
	Intermed.	-0.027±0.018	-0.027±0.012#	-0.038±0.015#	0.022±0.013#	0.015±0.005#
	High	-0.042±0.018†	**-0.040±0.012†**	-0.023±0.015	0.013±0.013	0.008±0.005†
OSI	Low	-0.029±0.017	-0.029±0.012	-0.021±0.015*	0.014±0.013	0.007±0.005
	Intermed.	**-0.042±0.017#**	-0.035±0.012	-0.030±0.015#	0.014±0.013#	0.009±0.005#
	High	-0.028±0.017	-0.034±0.012	-0.040±0.015†	0.026±0.013†	0.020±0.005†
RRT	Low	-0.041±0.018	-0.041±0.012	-0.026±0.015	0.018±0.013*	0.008±0.005
	Intermed.	-0.044±0.018#	-0.031±0.012	**-0.028±0.015#**	0.007±0.013#	0.008±0.005#
	High	-0.012±0.018†	-0.024±0.012†	-0.034±0.015†	0.027±0.013†	0.018±0.005†
CFI	Low	-0.035±0.018	-0.033±0.012	-0.022±0.015	0.015±0.013	0.004±0.005*
	Intermed.	-0.036±0.017	-0.030±0.012	-0.027±0.015#	0.011±0.013#	0.009±0.005#
	High	-0.025±0.018	-0.036±0.012	-0.041±0.015†	0.028±0.013†	0.023±0.005†
transWSS	Low	-0.041±0.017	-0.031±0.012	-0.026±0.015	0.009±0.012*	**0.007±0.005***
	Intermed.	-0.030±0.017	-0.032±0.012	-0.032±0.015	0.023±0.012	0.011±0.005#
	High	-0.026±0.017	-0.035±0.012	-0.029±0.015	0.02±0.012†	0.017±0.005†

Intermed.: intermediate. $p<0.05$: low versus intermediate (*), intermediate versus high (#) and low versus high (†).

$p>0.01$ and $p<0.05$: in bold.

Supplementary Table 4. Change in plaque area and composition (±the standard error) over a six-month period for plaques exposed to low or high time-averaged wall shear stress (TAWSS) co-localised with low, intermediate and high cross-flow index.

	CFI	Total plaque area (mm^2)	Fibrous tissue area (mm^2)	Fibrous-fatty area (mm^2)	Necrotic core area (mm^2)	Dense calcium area (mm^2)
Low TAWSS	Low	0.153±0.046	0.124±0.033	0.038±0.023	0.004±0.023	0.000±0.012
	Intermed.	0.103±0.038#	0.050±0.027#	0.033±0.021#	0.001±0.020	0.021±0.010
	High	-0.026±0.021†	-0.030±0.014†	-0.020±0.016†	0.027±0.014	0.018±0.006
High TAWSS	Low	-0.030±0.019	-0.037±0.012	-0.020±0.016	0.020±0.013*	0.006±0.005
	Intermed.	-0.046±0.019	-0.036±0.012#	-0.024±0.016#	**0.006±0.013#**	0.007±0.005#
	High	-0.054±0.020	-0.059±0.013†	-0.037±0.017†	0.018±0.013	0.022±0.006†

CFI: cross-flow index; Intermed.: intermediate. $p<0.05$: low versus intermediate (*), intermediate versus high (#) and low versus high (†).

$p>0.01$ and $p<0.05$: in bold.

Supplementary Table 5. Change in plaque area and composition (±the standard error) over a six-month period for plaques exposed to low or high time-averaged wall shear stress (TAWSS) co-localised with low, intermediate and high oscillatory shear index (OSI).

	OSI	Total plaque area (mm^2)	Fibrous tissue area (mm^2)	Fibrous-fatty area (mm^2)	Necrotic core area (mm^2)	Dense calcium area (mm^2)
Low TAWSS	Low	0.256±0.043*	0.184±0.031*	0.103±0.023*	-0.017±0.022	-0.002±0.011
	Intermed.	-0.003±0.048	-0.008±0.034	0.009±0.025#	-0.005±0.024	0.003±0.013
	High	-0.027±0.022†	-0.030±0.014†	-0.042±0.018†	**0.026±0.014†**	0.018±0.006
High TAWSS	Low	-0.025±0.019*	-0.036±0.012	-0.021±0.017*	0.021±0.013	0.010±0.005
	Intermed.	-0.058±0.020	-0.048±0.012	-0.031±0.017	0.013±0.013	0.007±0.005#
	High	**-0.047±0.019†**	-0.045±0.013	-0.029±0.017	0.012±0.013	0.014±0.006

Intermed.: intermediate. $p<0.05$: low versus intermediate (*), intermediate versus high (#) and low versus high (†).

$p>0.01$ and $p<0.05$: in bold.

Supplementary Table 6. Change in plaque area and composition (±the standard error) over a six-month period for plaques exposed to low or high time-averaged wall shear stress (TAWSS) co-localised with low, intermediate and high relative residence time (RRT).

	RRT	Total plaque area (mm^2)	Fibrous tissue area (mm^2)	Fibrous-fatty area (mm^2)	Necrotic core area (mm^2)	Dense calcium area (mm^2)
Low TAWSS	Low	--	--	--	--	--
	Intermed.	--	--	--	--	--
	High	-0.001±0.021	-0.012±0.014	-0.030±0.016	0.024±0.014	0.018±0.006
High TAWSS	Low	-0.043±0.018	-0.043±0.012	-0.024±0.016	0.017±0.013*	0.007±0.005
	Intermed.	-0.058±0.019#	-0.042±0.013#	-0.024±0.015	0.001±0.013#	0.006±0.005#
	High	0.014±0.021†	-0.013±0.015†	-0.014±0.016	0.024±0.014	0.018±0.006†

Intermed.: intermediate. $p<0.05$: low versus intermediate (*), intermediate versus high (#) and low versus high (†).